Reaction kinetics and growth window for plasma-assisted molecular beam epitaxy of Ga2O3: Incorporation of Ga vs. Ga2O desorption

Patrick Vogt and Oliver Bierwagen

Citation: Applied Physics Letters **108**, 072101 (2016); doi: 10.1063/1.4942002
View online: http://dx.doi.org/10.1063/1.4942002
View Table of Contents: http://scitation.aip.org/content/aip/journal/apl/108/7?ver=pdfcov
Published by the AIP Publishing

Reaction kinetics and growth window for plasma-assisted molecular beam epitaxy of Ga_2O_3: Incorporation of Ga vs. Ga_2O desorption

Patrick Vogt and Oliver Bierwagen[a)]
Paul-Drude-Institut für Festkörperelektronik, Hausvogteiplatz 5–7, D-10117 Berlin, Germany

(Received 18 December 2015; accepted 30 January 2016; published online 17 February 2016)

A detailed study of the reaction kinetics of the plasma-assisted molecular beam epitaxy (MBE) growth of the *n*-type semiconducting oxide Ga_2O_3 is presented. The growth rate as a function of gallium flux is measured *in situ* by laser reflectometry at different growth temperatures (T_G) and gallium-to-oxygen ratios (r_{Ga}). The flux of the suboxide Ga_2O desorbed off the growth surface is identified *in situ* by line-of-sight quadrupole mass spectroscopy. The measurements reveal the influence of T_G and r_{Ga} on the competing formation of Ga_2O_3 and desorption of Ga_2O resulting in three different growth regimes: (i) Ga transport limited, (ii) Ga_2O desorption limited, and (iii) O transport limited. As a result, we present a growth diagram of gallium oxide. This diagram illustrates the regimes of complete, partial, and no Ga incorporation as a function of T_G and r_{Ga}, and thus provides guidance for the MBE growth of Ga_2O_3. © *2016 AIP Publishing LLC*. [http://dx.doi.org/10.1063/1.4942002]

Transparent semiconducting oxides (TSOs) with relatively wide band gaps—such as gallium oxide, indium oxide, or tin dioxide—have generated much interest because of their intriguing electrical and optical properties.[1–3] Due to its large band gap of ~5 eV (Ref. 4), gallium sesquioxide (Ga_2O_3) is a promising material for deep ultra-violet detectors and high-power electronics.[5–7] These and other applications require a high degree of purity, crystallinity, and controlled doping, criteria which can be met in epitaxial thin film growth using pulsed laser deposition,[8] metal-organic chemical vapor phase epitaxy,[9] and ozone or plasma-assisted molecular beam epitaxy (MBE).[10–14] The highest-quality Ga_2O_3 single-crystal layers are grown using homoepitaxy on bulk crystals of Ga_2O_3, which are produced via the Czochralski,[15,16] edge-defined film-fed,[17,18] and floating zone[7] growth methods.

In plasma-assisted molecular beam epitaxy, Ga_2O_3 is grown by the oxidation of a flux of evaporated Ga (Φ_{Ga}) by a flux of plasma-activated oxygen (Φ_O) on a heated substrate. This growth is typically performed under oxygen-rich conditions with respect to the stoichiometry of the perfect crystal by providing more O than Ga atoms to the growth surface. This is in contrast to the growth of films of other Ga- or O-based semiconductors, such as GaN[19] or In_2O_3,[20] where metal-rich growth conditions yield improved structural properties. In addition, Ga-rich growth conditions are likely to help suppress the formation of Ga vacancies that act as compensating acceptors in Ga_2O_3.[21,22]

The Ga_2O_3 growth rate (Γ) is limited by Φ_{Ga} under O-rich growth conditions, and thus increases linearly with Φ_{Ga} up to the stoichiometric Ga flux (Φ_{SF}), which consumes all the available oxygen for Ga_2O_3 formation.[14]

Higher Ga fluxes (i.e., $\Phi_{Ga} > \Phi_{SF}$) push growth into the Ga-rich regime, where Γ decreases with increasing Φ_{Ga}. This decrease is due to the oxygen-deficiency-induced formation of the volatile suboxide Ga_2O, which desorbs rather than contributing to Ga_2O_3 formation.[14] Such a decreasing growth rate with increasing Ga flux has also been observed previously by Tsai *et al.*[13] In contrast, Oshima *et al.*[11] and Okumura *et al.*[10] have reported that the growth rate stays constant with increasing Φ_{Ga} in the Ga-rich regime. In addition to its dependence on Φ_{Ga}, Sasaki *et al.*[12] and Okumura *et al.*[10] have shown the growth temperature (T_G) to influence on the growth rate as well.

In this letter, we present a detailed, systematic study of the reaction kinetics involved in the MBE growth of Ga_2O_3. We show that the growth rate is governed by the competition between Ga_2O_3 accumulation and Ga_2O desorption as a function of T_G, Φ_{Ga}, and Φ_O. Based on this data, we develop a growth diagram that describes the growth window and different regimes of Ga incorporation as a function of both T_G and the Ga-to-O ratio ($r_{Ga} = \Phi_{Ga}/\Phi_O$). This diagram may guide the optimization of MBE growth conditions for the further improvement of Ga_2O_3 structures.

Textured, nonpolycrystalline β-$Ga_2O_3(\bar{2}01)$ with rotational domains[11] was grown on *c*-plane sapphire ($Al_2O_3(0001)$) in a custom made MBE system. Quarters of 2-inch diameter, single-side polished, *c*-plane sapphire wafers were used as the substrates for this study. The rough backside of the substrate was sputter-coated with titanium to improve substrate heating. During growth, the substrate temperature was measured with a pyrometer. A standard shuttered hot-lip effusion cell was used to evaporate liquid Ga (7N purity). A radio frequency plasma source with a mass flow controller supplied activated oxygen from the research-grade O_2 gas (6N purity). The beam equivalent pressure (BEP)—which is proportional to the particle flux—was measured by a nude filament ion gauge positioned at the substrate location, and then removed prior to growth. The radio frequency power of the plasma source was maintained at 300 W throughout Ga_2O_3 growth.

The Ga flux was calibrated by measuring the growth rate of the Ga_2O_3 layer in the O-rich regime and low T_G (i.e., no Ga_2O and/or Ga desorption). The O-rich regime was identified by measuring the growth rate as described below. With this calibration, we converted the measured BEPs into the equivalent Ga_2O_3 growth rates that are used throughout

a)Email: bierwagen@pdi-berlin.de

this study. The Ga flux ranged from $\Phi_{Ga} = 1.5 \times 10^{-7}$ Torr $\hat{=}$ 0.4 Å/s to 15×10^{-7} Torr $\hat{=}$ 4 Å/s. With O mass flows of 1 and 3, standard cubic centimeters per minute (SCCM), two different O fluxes of $\Phi_O = 1 \times 10^{-5}$ Torr $\hat{=}$ 1.7 Å/s and $\Phi_O = 3 \times 10^{-5}$ Torr $\hat{=}$ 5.1 Å/s, respectively, were used. Their calibration in Å/s was made by the growth rates at stoichiometric flux conditions. With these calibrations, we define our Ga-to-O ratio as $r_{Ga} = \Phi_{Ga}/\Phi_O$. It is equal to 1 at the stoichiometric flux condition.

All growth rates presented in this letter were measured by laser reflectometry.[14] Here, a laser with a wavelength of 650 nm was used. With an incidence angle between the laser and the growth surface of 30°, one oscillation period corresponded to a change of layer thickness by 180 nm. The suboxide (Ga_2O) flux desorbing off the growth surface (Φ_{Ga_2O}) was also measured by a line-of-sight quadrupole mass spectrometer (QMS),[23] which allowed the mass of the desorbing species to be identified. The QMS signal was converted into an equivalent growth rate by scaling it to match the supplied Ga flux under conditions of complete suboxide formation (with an appropriate O flux). The crystallinity of the oxide films was verified by a spotty reflection high energy electron diffraction (RHEED) pattern during growth (corresponding to transmission diffraction of the electron beam through the apex of the faceted film surface) and by post-growth X-ray diffraction ω–2θ wide-range scans (not shown).

The growth rate (Γ) of Ga_2O_3 and Φ_{Ga_2O} as functions of Φ_{Ga} at substrate temperatures of $T_G = 500$ °C and 660 °C are depicted in Fig. 1. At the low growth temperature ($T_G = 500$ °C) in the O-rich regime, i.e., at $r_{Ga} \leq 1$, the growth rate increases linearly with Φ_{Ga}. Since no desorbed signal could be detected by QMS, the entire Ga is fully incorporated into the film (unity sticking coefficient in this case).[14] After reaching a maximum at $r_{Ga} = 1$, growth enters the Ga-rich regime and Γ shows a linear decrease due to suboxide formation (as described in Ref. 14). The flux of desorbing suboxide could then be detected by QMS and is depicted as black circles in the plot in Fig. 1.

Identical fluxes result in a different evolution of the growth rate when a higher substrate temperature of 660 °C as shown by the open, blue symbols in Fig. 1 is used. The maximum growth rate is decreased in comparison to growth at $T_G = 500$ °C. Additionally, Γ forms a plateau in the O-rich regime, which resembles the Γ evolution reported in Refs. 11 and 10 for the MBE growth of Ga_2O_3 on Al_2O_3(0001) and Ga_2O_3(010), respectively. QMS measurements reveal that this plateau arises due to Ga_2O formation. The reactions for the layer growth and suboxide formation are

$$2\mathrm{Ga}(g) + 3\mathrm{O}(g) \rightarrow \mathrm{Ga_2O_3}(s), \quad (1)$$

and

$$2\mathrm{Ga}(g) + 1\mathrm{O}(g) \rightarrow \mathrm{Ga_2O_1}(g). \quad (2)$$

The labels g and s denote the gas and solid phase, respectively. The open and filled diamonds in Fig. 1 give the sum of $\Gamma + \Phi_{Ga_2O}$ for both growth temperatures. This sum is equal to Φ_{Ga}, proving that the difference between Ga flux and Ga_2O_3 growth rate is solely due to suboxide desorption. Note that no Ga desorption was detected, indicating it is not responsible for the plateau in the growth rate. In a separate experiment, we observed Ga desorption instead of Ga_2O desorption when Ga and O fluxes of 1.6 and 1.7 Å/s, respectively, were supplied to a blank Al_2O_3(0001) surface at similarly high temperatures between 900 and 550 °C. The different Ga species desorbing from the Al_2O_3 and Ga_2O_3 surfaces suggest that the Ga_2O_3 surface is required as a catalyst for Ga_2O formation.

It is significant that a higher O flux resulted in a correspondingly higher maximum Γ, as shown by the red star in Fig. 1. This suggests that the growth rate may be normalized by the flux of active O, i.e., $r_\Gamma = \Gamma/\Phi_O$. In Fig. 2, the normalized growth rate (r_Γ) is plotted as a function of r_{Ga} for four different growth temperatures. It shows the same evolution as in Fig. 1. For $T_G > 500$ °C, a plateau in the O-rich regime and a decrease of r_Γ are present. Additionally, we observe that in the O-rich regime, the maximum normalized growth rate β (position of the plateau in Fig. 2) decreases with increasing T_G. The temperature dependence of β is

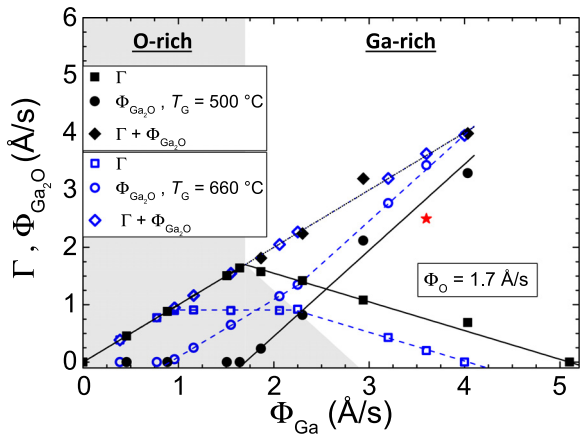

FIG. 1. Ga_2O_3 growth rate (Γ), Ga_2O desorption rate (Φ_{Ga_2O}), and their sum shown as a function of Φ_{Ga} at constant O flux of 1.7 Å/s at two different growth temperatures (T_G). The lines are guides for the eye. The red star corresponds to the growth rate at a high temperature $T_G = 660$ °C and a higher O flux of $\Phi_O = 5.1$ Å/s.

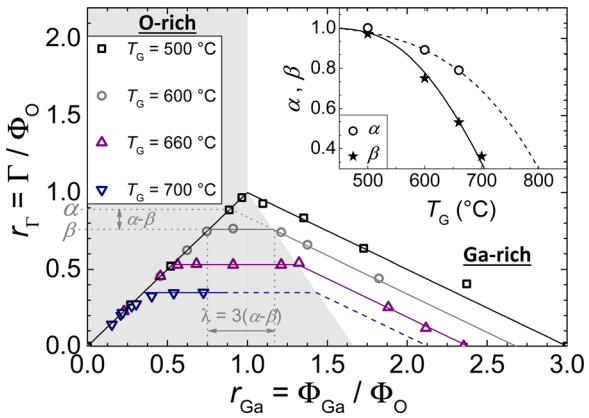

FIG. 2. Growth rates normalized by the O flux ($r_\Gamma = \Gamma/\Phi_O$) as a function of the Ga-to-O ratio (r_{Ga}) for four different growth temperatures. The supplied active O flux was 1.7 Å/s for $T_G = 500$, 600, 660 °C and 5.1 Å/s for 700 °C. The growth rate evolution is parametrized by the maximum growth rate (β) and the O flux (α) that may react with Ga (to form Ga_2O_3 or Ga_2O), normalized by the active O flux. Inset: the influence of T_G on α and β. The lines are guides for the eye.

depicted in the inset of Fig. 2. Furthermore, the inset shows the fraction of the maximum O flux that is available to react with Ga (to Ga_2O_3 or Ga_2O), denoted by α. The value of α is calculated by extending the growth rate evolution from the Ga-rich regime until it intersects the curve in the O-rich regime (see the dotted gray line for $T_G = 600\,^{\circ}C$, for example).

The width of the plateau is determined by the remaining active O atoms that are not incorporated into the Ga_2O_3 layer, but instead react to form Ga_2O. Since only one O atom is needed to form Ga_2O—instead of the three needed for Ga_2O_3—the width of the plateau in Γ is $\lambda = 3(\alpha - \beta)$. The plateau at a given T_G covers the range of r_{Ga} from β to $\beta + \lambda$. Once all active O atoms are consumed by reactions (1) and (2), growth shifts into the Ga-rich regime. Here, the growth rate decreases due to insufficient O atoms to oxidize the Ga to Ga_2O_3. Finally, the growth stops at a Ga flux three times the stoichiometric flux, as all available Ga and O are consumed by the formation of Ga_2O (i.e., at a Ga-to-O ratio of $r_{Ga} = 3\alpha$).

Now, we give the reactions for three growth regimes, which we define as follows: (i) Ga transport limited O-rich growth with full Ga incorporation (the linear increase of r_Γ with r_{Ga}), (ii) Ga_2O desorption limited O-rich growth with partial Ga incorporation (the plateau of r_Γ), (iii) O transport limited Ga-rich growth with partial Ga incorporation (the decrease of r_Γ with r_{Ga}).

For regime (i) (i.e., for $0 \le r_{Ga} < \beta \le 1$), the reaction is

$$r_{Ga}\,2\mathrm{Ga}(g) + 3\mathrm{O}(g) \rightarrow r_{Ga}\mathrm{Ga_2O_3}(s) + 3(1 - r_{Ga})\mathrm{O}(g). \tag{3}$$

The plateau of regime (ii) ($0 < \beta \le r_{Ga} \le \beta + \lambda = 3\alpha - 2\beta$) is described by the reaction

$$\begin{aligned} r_{Ga}\,2\mathrm{Ga}(g) + 3\mathrm{O}(g) &\rightarrow \beta\mathrm{Ga_2O_3}(s) \\ &+ (r_{Ga} - \beta)\mathrm{Ga_2O}(g) + (3 - r_{Ga} + 2\beta)\mathrm{O}(g). \end{aligned} \tag{4}$$

The end of the plateau ($r_{Ga} = \beta + \lambda$) corresponds to the stoichiometric growth conditions. For Ga-rich growth in regime (iii) ($\beta + \lambda < r_{Ga} \le 3\alpha$), the growth rate decreases and

$$\begin{aligned} r_{Ga}\,2\mathrm{Ga}(g) + 3\mathrm{O}(g) &\rightarrow \beta\gamma\mathrm{Ga_2O_3}(s) \\ &+ (r_{Ga} - \beta\gamma)\mathrm{Ga_2O}(g) + 3(1 - \alpha)\mathrm{O}(g). \end{aligned} \tag{5}$$

The coefficient γ decreases linearly with increasing r_{Ga}, from unity at $r_{Ga} = \beta + \lambda = 3\alpha - 2\beta$ to zero at $r_{Ga} = 3\alpha$, i.e., $\gamma = -(2\beta)^{-1}(r_{Ga} - 3\alpha)$.

Practical information for the MBE growth of Ga_2O_3 is included in Fig. 3, which depicts the growth rate normalized by the maximum growth rate, $\rho = \Gamma/\Gamma^{max}$, as a function of T_G. Here, the temperature evolution of ρ for five different Ga-to-O ratios ranging from 0.18 (O-rich) to 1.65 (Ga-rich) is plotted. For all five data sets, the growth rate decreases with increasing growth temperature. The constant growth rate at low T_G is reflected by reaction (3) for $r_{Ga} \le 1$ (regime (i)) and reaction (5) for $r_{Ga} > 1$ with $\alpha = \beta = 1$ (regime (iii)). The decreasing growth rate at higher T_G for $r_{Ga} \le 1$ and $\beta < 1$ is described by the plateau (reaction (4), regime (ii)) and reaction (5) for $r_{Ga} > 1$ and $\alpha < 1$ (regime (iii)). No layer growth occurs at growth temperatures when $\beta = 0$ for

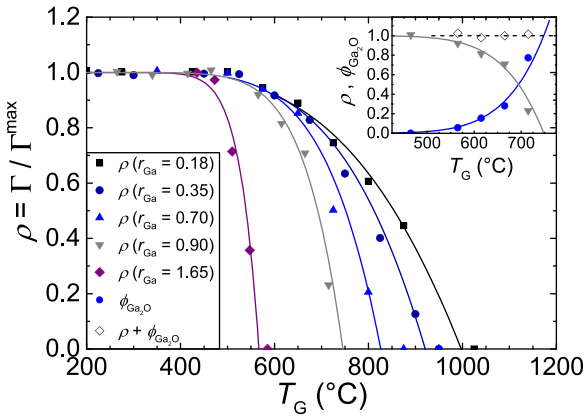

FIG. 3. Relative change of the growth rates with increasing T_G for five different Ga-to-O ratios r_{Ga}. The O flux supplied was 1.7 Å/s for $r_{Ga} = 0.90, 1.65$ and 5.1 Å/s for $r_{Ga} = 0.18, 0.35, 0.70$. Inset: ρ versus T_G for $r_{Ga} = 0.90$ (triangles), the desorbed suboxide flux normalized by maximum growth rate ϕ_{Ga_2O} (circles), and their sum (open rhombs). The lines are guides for the eye.

$r_{Ga} \le 1$, and/or $\alpha = 0$ for $r_{Ga} > 1$, and additionally, for $r_{Ga} > 3\alpha$.

The inset in Fig. 3 exemplarily shows the temperature dependence of ρ for $r_{Ga} = 0.90$ at temperatures below 750 °C. Furthermore, the normalized desorption rate $\phi_{Ga_2O} = \Phi_{Ga_2O}/\ \Gamma^{max}$ is plotted in the same temperature range. Their sum equals unity for all growth temperatures, again confirming a reduced growth rate at higher T_G due to volatile Ga_2O formation catalyzed by the Ga_2O_3 layer.

By combining the results in Figs. 1–3, we conclude that a higher r_{Ga} and T_G promote the formation and desorption of Ga_2O, but that they can also result in a stabilized Ga_2O_3 growth rate at sufficiently high T_G. The detailed regimes (i)–(iii) can describe all growth rate scenarios in this study (Figs. 1–3) and those reported in the literature for homo- and heteroepitaxial growth.[10–14,24]

By merging all data shown in Figs. 1–3, we derive a Ga_2O_3 growth diagram (GD) using controllable experimental parameters Φ_{Ga}, Φ_O, and T_G, as shown in Fig. 4. It depicts the three growth regimes (i)–(iii) as explained above. The growth window is formed by the union of these three

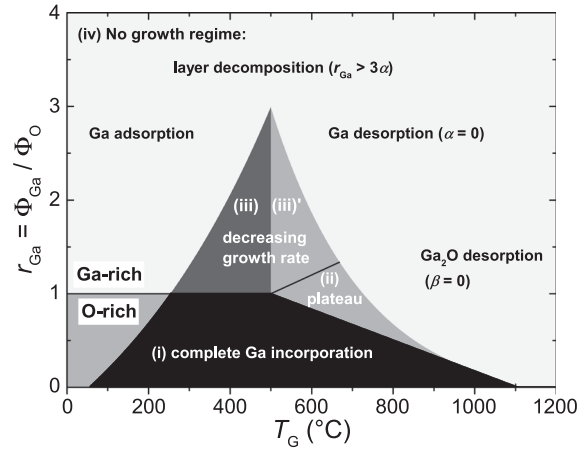

FIG. 4. A growth diagram (GD) for the Ga_2O_3 MBE growth including all experimental parameters (Φ_{Ga}, Φ_O) and T_G. It is divided into two major regimes: O-rich and Ga-rich. The GD illustrates regimes of complete (i), partial (ii, iii, iii′), and no Ga-incorporation (iv) as a function of T_G and r_{Ga}.

regimes. Note that in Fig. 4, in addition to regime (iii) where $\alpha = 1$, in the regime (iii)′, the oxygen desorption $\alpha < 1$ is taken into account. Here, the oxygen density on the growth surface is lower than in (iii) ($\alpha < 1$), and therefore, the maximum growth rate at a given r_{Ga} in the Ga-rich regime is decreased. Both scenarios are described by reaction (5). In addition, this diagram shows the no growth regime (iv), which includes all possible no growth scenarios: full Ga adsorption, full Ga desorption, and layer decomposition by etching as described in Ref. 14.

This GD may be qualitatively applied for other Ga_2O_3 surfaces. The difference in adhesion energies of the Ga adatoms at the various Ga_2O_3 surfaces would result in a growth temperature shift in the GD. The shape of the growth diagram remains the same due to the preserving stoichiometry (i.e., two Ga atoms and three O atoms).

In summary, we have studied the growth rate evolution of the heteroepitaxial growth of $Ga_2O_3(\bar{2}01)$ on $Al_2O_3(0001)$ by plasma-assisted molecular beam epitaxy, and the competing desorption of Ga_2O. The growth rate and desorbed flux were measured *in situ* by laser reflectometry and line-of-sight quadrupole mass spectroscopy, respectively. The Ga flux, Ga-to-O ratio, and growth temperature were systematically varied in order to understand the reaction kinetics of the Ga_2O_3 growth. By combining our results, we developed a growth diagram with three distinctive growth regimes: (i) complete Ga incorporation (i.e., Ga transport limited growth regime (O-rich)), (ii) plateau of growth rate at increasing Ga flux (i.e., Ga_2O desorption limited growth regime (O-rich)), (iii) a decreasing growth rate at increasing Ga flux (i.e., O-transport-limited growth regime (Ga-rich)). In all the cases, the difference between the provided Ga flux and the growth rate is related to the formation and desorption of the volatile Ga_2O, which is catalyzed by the Ga_2O_3 surface. No Ga desorption was observed at the investigated growth temperatures. Growth rates lower than the Ga flux were either caused by the growth in the Ga-rich regime or by a higher growth temperature. These findings are likely applicable to ozone MBE. In addition, we speculate that Ga_2O desorption may also play a role in the growth of Ga_2O_3 by metal-organic chemical vapor deposition.

Our results give guidance for the improvement of growth rates, crystal quality, and electronic structure during Ga_2O_3 growth. For example, higher growth rates on the $Ga_2O_3(100)$ surface may be realized by lower growth temperatures that suppress Ga_2O desorption. In order to improve crystal quality, high-temperature growth is needed, and our results reveal that an increased O flux helps maintain reasonable growth rates in this case. In the plateau regime, the growth rate is Ga flux-independent when the growth temperature is stable. Finally, growth in this regime and more in the Ga-rich regime may suppress the formation of Ga vacancies, which are responsible for the compensation of electrical donors.

We would like to thank Hans-Peter Schönherr for technical MBE support and Vladimir Kaganer for critically reading the manuscript. We would also like to thank Joseph M. Wofford for proofreading the manuscript.

[1]O. Bierwagen, Semicond. Sci. Technol. **30**, 024001 (2015).
[2]Z. Galazka, R. Uecker, D. Klimm, K. Irmscher, M. Pietsch, R. Schewski, M. Albrecht, A. Kwasniewski, S. Ganschow, D. Schulz, C. Guguschev, R. Bertram, M. Bickermann, and R. Fornari, Phys. Status Solidi A **211**, 66 (2014).
[3]T. Oshima, K. Matsuyama, K. Yoshimatsu, and A. Ohtomo, J. Cryst. Growth **421**, 23 (2015).
[4]C. Janowitz, V. Scherer, M. Mohamed, A. Krapf, H. Dwelk, R. Manzke, Z. Galazka, R. Uecker, K. Irmscher, R. Fornari, M. Michling, D. Schmeißer, J. R. Weber, J. B. Varley, and C. G. Van De Walle, New J. Phys. **13**, 085014 (2011).
[5]M. Higashiwaki, K. Sasaki, A. Kuramata, T. Masui, and S. Yamakoshi, Appl. Phys. Lett. **100**, 013504 (2012).
[6]M. Orita, H. Ohta, M. Hirano, and H. Hosono, Appl. Phys. Lett. **77**, 4166 (2000).
[7]Y. Tomm, J. M. Ko, A. Yoshikawa, and T. Fukuda, Sol. Energy Mater. Sol. C **66**, 369 (2001).
[8]D. Splith, S. Müller, F. Schmidt, H. von Wenckstern, J. J. van Rensburg, W. E. Meyer, and M. Grundmann, Phys. Status Solidi A **211**, 40 (2014).
[9]G. Wagner, M. Baldini, D. Gogova, M. Schmidbauer, R. Schewski, M. Albrecht, Z. Galazka, D. Klimm, and R. Fornari, Phys. Status Solidi A **211**, 27 (2014).
[10]H. Okumura, M. Kita, K. Sasaki, A. Kuramata, M. Higashiwaki, and J. S. Speck, Appl. Phys. Express **7**, 095501 (2014).
[11]T. Oshima, T. Okuno, and S. Fujita, Jpn. J. Appl. Phys., Part 1 **46**, 7217 (2007).
[12]K. Sasaki, M. Higashiwaki, A. Kuramata, T. Masui, and S. Yamakoshi, J. Cryst. Growth **392**, 30 (2014).
[13]M.-Y. Tsai, O. Bierwagen, M. E. White, and J. S. Speck, J. Vac. Sci. Technol., A **28**, 354 (2010).
[14]P. Vogt and O. Bierwagen, Appl. Phys. Lett. **106**, 081910 (2015).
[15]Z. Galazka, R. Uecker, K. Irmscher, M. Albrecht, D. Klimm, M. Pietsch, M. Brützam, R. Bertram, S. Ganschow, and R. Fornari, Cryst. Res. Technol. **45**, 1229 (2010).
[16]Y. Tomm, P. Reiche, D. Klimm, and T. Fukuda, J. Cryst. Growth **220**, 510 (2000).
[17]H. Aida, K. Nishiguchi, H. Takeda, N. Aota, K. Sunakawa, and Y. Yaguchi, Jpn. J. Appl. Phys., Part 1 **47**, 8506 (2008).
[18]M. Higashiwaki, K. Sasaki, A. Kuramata, T. Masui, and S. Yamakoshi, Phys. Status Solidi A **211**, 21 (2014).
[19]E. Calleja, M. A. Sánchez-García, F. J. Sánchez, F. Calle, F. B. Naranjo, E. Muñoz, S. I. Molina, A. M. Sánchez, F. J. Pacheco, and R. García, J. Cryst. Growth **201**, 296 (1999).
[20]O. Bierwagen, M. E. White, M.-Y. Tsai, and J. S. Speck, Appl. Phys. Lett. **95**, 262105 (2009).
[21]E. Korhonen, F. Tuomisto, D. Gogova, G. Wagner, M. Baldini, Z. Galazka, R. Schewski, and M. Albrecht, Appl. Phys. Lett. **106**, 242103 (2015).
[22]J. B. Varley, J. R. Weber, A. Janotti, and C. G. Van de Walle, Appl. Phys. Lett. **97**, 142106 (2010).
[23]S. Fernández-Garrido, J. K. Zettler, L. Geelhaar, and O. Brandt, Nano Lett. **15**, 1930 (2015).
[24]K. Sasaki, A. Kuramata, T. Masui, E. G. Víllora, K. Shimamura, and S. Yamakoshi, Appl. Phys. Express **5**, 035502 (2012).